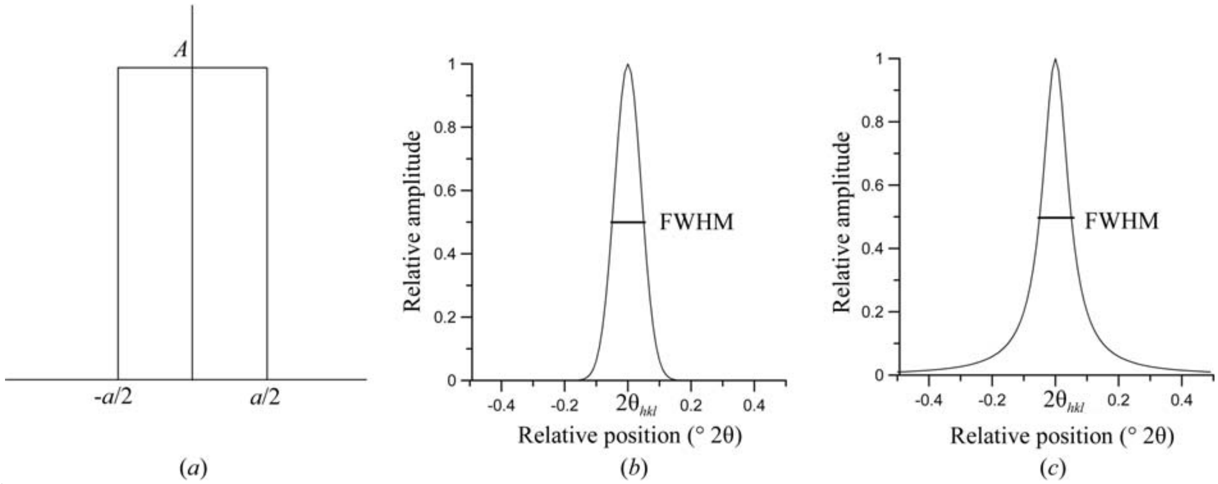

Figure 1.1.18
Normalized peak-shape functions. (*a*) The hat function, (*b*) the Gaussian function and (*c*) the Lorentzian function.

1.1.4. The peak profile

The peak profile refers to the shape of the measured Bragg peak. In the treatment above, the Bragg peaks from a perfect infinite crystal were delta functions and therefore infinitely narrow. In reality, the finite size of the crystal, the finite resolution of the measurement and defects in the material that result in inhomogeneous strains all broaden the delta function, giving it a finite width and some characteristic shape. When fitting a model to the measured diffraction pattern we should correctly account for these effects in order to obtain correct values for the Bragg-peak intensities. On the other hand, a careful study of the peak shapes yields important information about the size of the crystallites in the sample and defects that they contain. With recent improvements in instrumentation and computational data-analysis methods, this latter type of study has become more important and is having considerable scientific and technological impact.

The convolution theorem of the Fourier transform that was introduced in the derivation of the crystallographic structure factor above is also very useful in understanding the peak profile. In this case, the measured Bragg peak can be thought of as a delta function convoluted with a profile (Klug & Alexander, 1974). The profile of the Bragg reflection hkl, Φ_{hkl}, can be written as

$$\Phi_{hkl}(2\theta_i - 2\theta_{hkl}) = \mathrm{EP}(2\theta_i) \otimes \mathrm{IP}(2\theta_i) \otimes \mathrm{MS}(2\theta_i - 2\theta_{hkl}), \quad (1.1.59)$$

where $\mathrm{EP}(2\theta_i)$ is the emission profile of the X-ray source (tube or synchrotron), $\mathrm{IP}(2\theta_i)$ contains additional contributions to the profile from the instrument and $\mathrm{MS}(2\theta_i - 2\theta_{hkl})$ is the contribution from the microstructure of the sample. The symbol $\otimes$ denotes convolution.

The convolution of two functions $f(t)$ and $g(t)$ in real space is defined as

$$(f \otimes g)(t) = \int\limits_{\tau=-\infty}^{\infty} f(\tau) g(t-\tau)\,\mathrm{d}\tau. \quad (1.1.60)$$

The convolution theorem tells us that the Fourier transform (FT) of two convoluted functions is the product of the Fourier transforms of those functions:

$$\mathrm{FT}(f \otimes g)(t) = \big(\mathrm{FT}(f)\big)\big(\mathrm{FT}(g)\big). \quad (1.1.61)$$

Normalization of the transform leads to scaling factors like 2π which have been omitted here for simplicity.

In practice, numerical integrations are almost always required, as many of the instrument aberration functions cannot be convoluted analytically. This convolution approach is the basis of the so-called fundamental-parameter (FP) approach (Cheary & Coelho, 1992) and has proven to be superior to other more empirical or phenomenological methods. The idea behind the FP approach is to build up the profile from first principles, exclusively using measurable physical quantities like slit widths, slit lengths, Soller-slit opening angles *etc*. The process of convolution from a fundamental-parameters perspective is an approximation whereby second- and higher-order effects are typically neglected for computational speed and simplicity. The instrumental profile is usually fully characterized by measuring a line-profile standard such as NIST SRM 660c LaB_6, which is expected to contain only small microstructural contributions, and comparing the calculated diffraction pattern to the measured one. Once the instrumental part of the profile is sufficiently well determined, it can be assumed that the remaining contributions to the 'real' profile are purely sample dependent (*e.g.* domain size, strain).

In general, it is desirable to keep the number of functions that are used to describe the peak profile to a minimum. Typical examples of mathematical functions which are convoluted to form the profile of a Bragg reflection include:

(*a*) the hat function H (*e.g.* for all kinds of rectangular slits),

$$H(2\theta - 2\theta_{hkl}) = \begin{cases} A \text{ for } -a/2 < (2\theta - 2\theta_{hkl}) < a/2, \\ 0 \text{ for } (2\theta - 2\theta_{hkl}) \le -a/2 \\ \quad \text{and } (2\theta - 2\theta_{hkl}) \ge -a/2 \end{cases} \quad (1.1.62)$$

(Fig. 1.1.18*a*);

(*b*) the normalized Gaussian G (*e.g.* for microstrain broadening),

$$G(2\theta - 2\theta_{hkl}) = \left(\frac{2\sqrt{\ln(2)/\pi}}{\mathrm{FWHM}}\right) \exp\left(\frac{-4\ln(2)(2\theta - 2\theta_{hkl})^2}{\mathrm{FWHM}^2}\right), \quad (1.1.63)$$

(Fig. 1.1.18*b*), where FWHM denotes the full width at half maximum of the Gaussian function in $^\circ\, 2\theta$; and

(*c*) the Lorentzian function L (*e.g.* for the emission profile),

$$L(2\theta - 2\theta_{hkl}) = \frac{1}{2\pi}\left(\frac{\mathrm{FWHM}}{(2\theta - 2\theta_{hkl}) + \mathrm{FWHM}^2/4}\right), \quad (1.1.64)$$

(Fig. 1.1.18*c*).